Dynamical evolution of sand ripples under water

Alexandre Stegner[1] and José Eduardo Wesfreid[2]

[1]*Laboratoire de Météorologie Dynamique, ENS, 24 Rue Lhomond, 75231 Paris, France*

[2]*Laboratoire de Physique et Mécanique des Milieux Hétérogènes (CNRS UMR No. 7636), ESPCI, 10 rue Vauquelin, 75231 Paris, France*

We have performed an experimental study on the evolution of sand ripples formed under the action of an oscillatory flow. An annular sand-water cell was used in order to investigate a wide range of parameters. The sand ripples follow an irreversible condensation mechanism from small to large wavelength until a final state is reached. The wavelength and the shape of these stable sand patterns are mainly governed by the fluid displacement and the static angle of the granular media. A strong hysteresis affects the evolution of steep ripples. When the acceleration of the sand bed reaches a critical value, the final pattern is modified by the superficial fluidization of the sand layer. [S1063-651X(99)50110-4]

PACS number(s): 47.54.+r, 45.70.Mg, 47.20.−k, 92.10.Wa

It is always fascinating to observe, along many coasts, the regular patterns (tens of centimeters in wavelength) formed on sandy sea beds. The destabilization of a flat sand surface under an oscillating flow is a generic mechanism producing periodic patterns. For instance, surface waves, which are known to induce a back and forth motion on the sea bed, are responsible for the formation of beach ripples. Although the formation of these patterns has been studied for a long time, the existence of stable patterns and the dominant wavelength selection mechanism are still unclear.

In the pioneering work of Bagnold [1] two types of ripples were distinguished. One called ''rolling-grain'' ripples characterized by the absence of flow separation behind the crest, the other one referred to as ''vortex'' ripples characterized by the existence of vortex shedding at the crest. In the first stage of growth, the ripple amplitude is so small that vortex formation is inhibited. In this case, steady recirculating cells, which can transport sand from the valley to the crest, appear above the wavy bottom [2]. Hence, the wavelength selection of ''rolling-grain'' ripples can be explained using a standard linear stability analysis and their shape predicted by a weak nonlinear analysis [3]. A similar theoretical approach was used to study the formation of large sand waves (a few hundred meters in wavelength) created in a shallow sea under the action of tidal flow [4]. However, the wavelength predicted by this approach should be observed in nature only if sand patterns having a small height-to-length ratio could reach an equilibrium state. In the case of beach ripples, field observation showed that their height-to-length ratio is in general larger than 0.1 and therefore the above condition could not be satisfied. In addition, the stationarity of small ripple perturbations in laboratory experiments remains ambiguous. Indeed, previous experiments [5] claim the existence of stable ''rolling-grain'' ripples, while in a recent work where the phase diagram of ripples was investigated [6] there is no stable region for small amplitude patterns. On the other hand, experiments on ''vortex'' ripples [1,7] have shown that the wavelength λ of steep sand patterns is proportional to the total amplitude L of the fluid oscillation: $\lambda = (2/3)L$ (henceforth ''2/3 law'') and neither depends on the frequency of the oscillation nor on the sand-grain density. The present work focuses on the long time

dynamic of sand ripples and characterizes with great accuracy the steady states reached by the system.

As recent experiments on sand ripples induced by an oscillating flow [6] or by a steady shear flow [8], we used a cylindrical geometry to achieve a quasi-one-dimensional system and to avoid end effects which could influence the destabilization of the sand bed. We took an annular channel, previously used for centrifugal instability studies (Fig. 1 in [9]), made of an inner black cylinder having a radius $R_1 = 6.925$ cm linked with an outer Plexiglas cylinder of radius $R_1 = 7.70$ cm, which gave a gap width of $a = 7.75$ mm. We closed the top and the bottom of the cell by rigid disks fixed to the cylinders. At the bottom of the cell we introduced a flat layer (7 cm height) of spherical glass particle having a mean diameter $d = 190$ μm and a density $\rho = 2.49$ kg/l^{-1} while the whole cell (29 cm height) is filled with water. An ac Servomotor in association with a Servopack controller was used to drive the whole cell. The two experimental parameters that govern the displacement $D(t) = (L/2)\cos(2\pi ft)$ of the annular channel, the frequency f and the amplitude of the oscillation $L/2$, were then easily regulated. The frequency was sufficiently high (from 0.2 to 2 Hz) to keep the Stokes layer $\delta = \sqrt{\nu/(\pi f)}$ (from 0.4 to 1 mm) smaller than the gap of the channel. If the inertial force $\rho_{sand} a_i$ [with $a_i = L/2(2\pi f)^2$] remains small compared with the effective gravity force acting on the sand grain ($\rho_{sand} - \rho_{water})g$, the dynamical behavior of the sand layer is expected to be identical whether the sand bed is stationary and the fluid moving or the fluid stationary and the bed moving. In order to satisfy this condition, we checked that the acceleration parameter $\Gamma_{water} = \rho_{sand} a_i / (\rho_{sand} - \rho_{water})g$ remained small (between 0.05 and 0.2). Therefore, as in previous studies [1,5–7], this experiment corresponds to a sand bed oscillating in still water. Also, the amplitude of oscillation was kept below the onset of the centrifugal instability that could occur between the cylinders [9].

The typical evolution of an initially flat sand bed, destabilized under the action of an oscillatory flow, is shown in Fig. 1. Using the relative motion of a (video) camera and the annular cell we reconstructed the ripple patterns along the whole circumference from a spatiotemporal record. This record took about 15 s; therefore, this technique was accurate
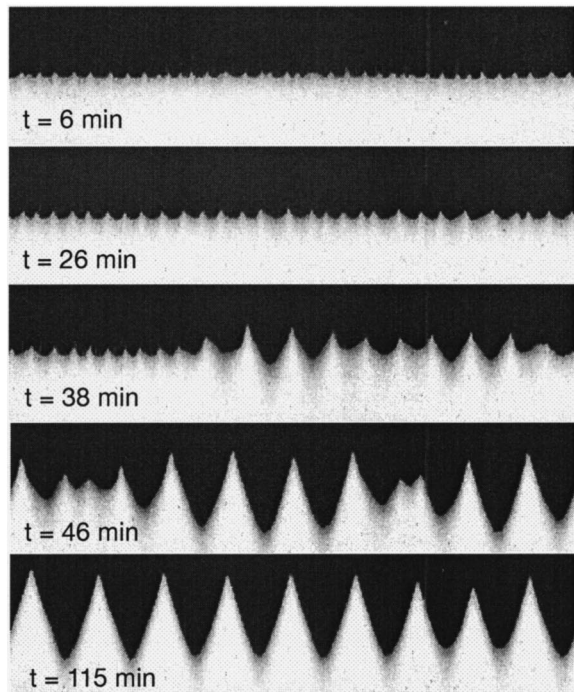
(a)
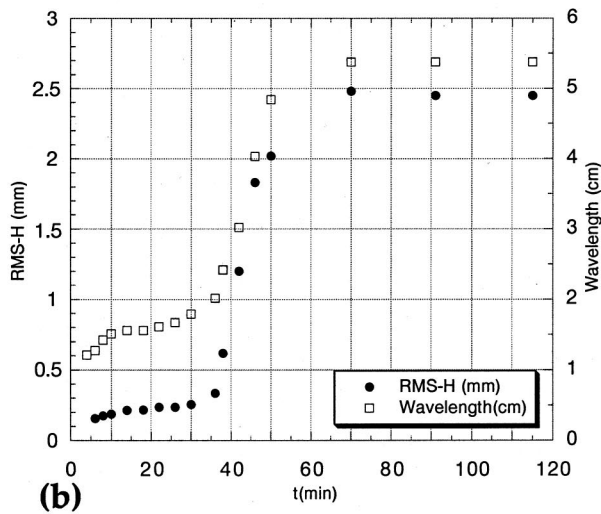
(b)

FIG. 1. Evolution of the shape (a), the root mean square amplitude and the mean wavelength (b) of a sand-bed pattern under an oscillatory flow ($L=8.06$ cm, $f=0.5$ Hz). The vertical scale is multiplied by 9 with respect to the horizontal scale for the images (a).

only for sand ripples having a slow evolution compared with the fluid oscillation. We measured, after video processing, the height profile of the sand patterns within an accuracy of 0.1 mm. Then, from the profile we extracted the root mean square of the height disturbance rms(h) and a mean wavelength λ both averaged around the perimeter. The evolution of these two quantities, corresponding to the patterns in Fig. 1(a) ($L=8.06$ cm and $f=0.5$ Hz), is shown in Fig. 1(b). According to these observations, a first disturbance, larger than the grain size, appears with a well defined wavelength on the flat bed. Then, both the amplitude and the wavelength increase continuously until a quasistationary state is reached.
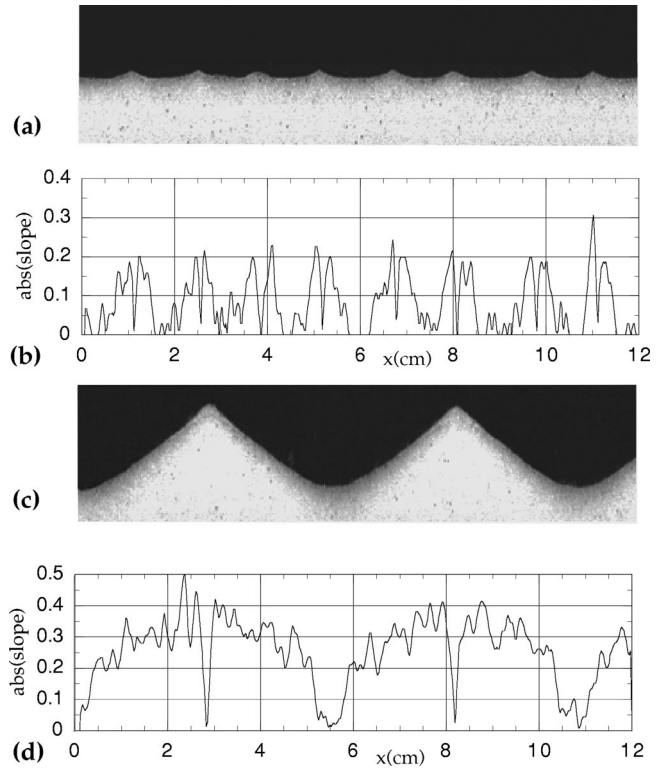

FIG. 2. Shape (a) and absolute value of the slope (b) of transient "rolling-grain" ripples ($L=8.06$ cm, $f=0.5$ Hz, and $t=14$ min) compared with the shape (c) and the absolute value of the slope (d) of the final steady "vortex" ripples (L,f idem while $t=115$ min). The vertical scale is multiplied by 2 with respect to the horizontal scale for the images (a) and (c).

At this stage, the sand patterns seem to saturate at a given wavelength but a slow growth in the amplitude can still be detected. The amplitude and the shape [see Fig. 2(a)], of these transient patterns correspond to "rolling-grain" ripples. However, if we wait long enough the system evolves to a final steady state. In all the cases we studied, even for very small oscillations, we observed the emergence of steep "vortex" ripples. For a strong forcing, the intermediate saturation disappears and the sand bed reaches its final state directly. Hence, "rolling-grain" ripples appear to be only transient or unstable patterns. For weak oscillation, the time needed to reach the final state can be very long, 10–14 days for instance when $L=2.9$ cm and $f=1$ Hz. This could explain why, if one did not wait long enough, weak amplitude ripples appeared to be steady in some previous experiments [1,5]. Besides, neglecting the long time evolution could also affect the determination of the onset of ripple formation. For instance, the above mentioned case ($L=2.9$ cm, $f=1$ Hz) is in the stable region of the phase diagram obtained in [6], because no ripples can be detected after half an hour of oscillation.

Starting from a flat bed, the wavelength of the final steady pattern depends only on the amplitude of the fluid oscillation Fig. 3(a). We recover here, for a wide range of parameters, the "2/3 law." Due to the annular geometry of the channel, it is necessary to choose L so that $2\pi R/\lambda$ is an integer, in order to get a final steady state without defects and with a well defined wavelength. However, if we start with an al-
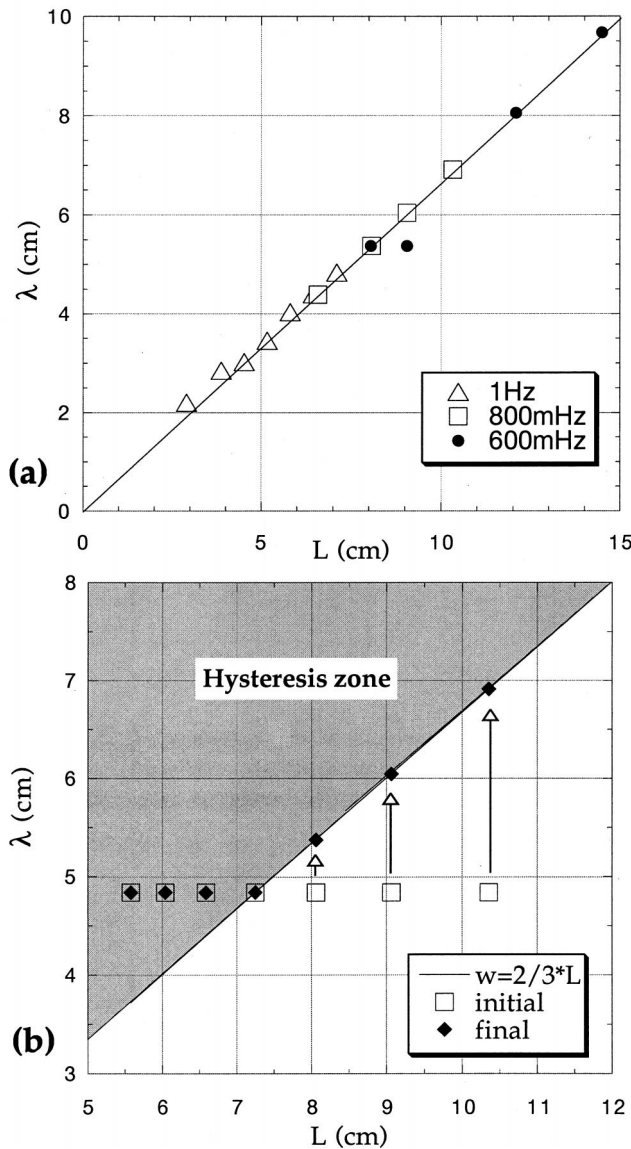
FIG. 3. Wavelength of the steady final pattern as a function of the total excursion of the fluid L. The solid line corresponds to the 2/3 law. In (a) we started the oscillation from an initially flat sand bed. In (b) we fixed the frequency to 0.6 Hz and we started the oscillation from a ripple bed of wavelength $\lambda = 4.8$ cm corresponding to the final state of a previous forcing with $L = 7.2$ cm.

ready rippled bed (a previous ''vortex'' ripple state) a strong hysteresis may appear. For a given L, if the wavelength of the initial state is smaller than $(2/3)L$ the sand pattern will evolve to reach the final state predicted by the ''2/3 law,'' whereas if the initial wavelength is larger than $(2/3)L$, the sand pattern will remain unchanged, as shown in Fig. 3(b). In other words, the relaxation of stable ripple patterns from large to small wavelength is not possible. Hence, this hysteresis may lead to a significant deviation from the ''2/3 law'' especially if the amplitude of the fluid oscillation changes in time.

Measurements of the local slope, at each point of the ripple profile, was obtained from a linear regression over 11 neighboring points. It indicates that the ripples slope is limited to a maximum value. This maximum slope $\tan \varphi_{max} = 0.37 \pm 0.03$ is always reached at the final stage of evolution
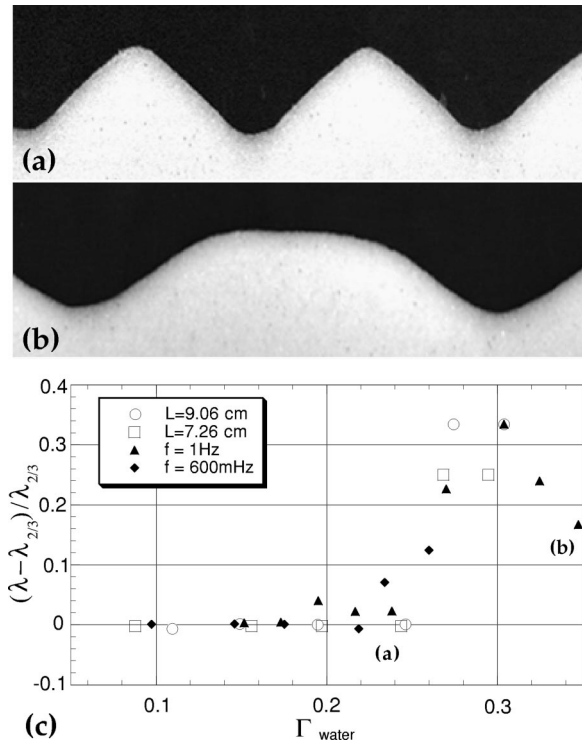

FIG. 4. Shapes of sinusoidal ripples (a) just before the bifurcation ($L = 7.1$ cm, $f = 1$ Hz, and $\Gamma_{water} = 0.24$) and squashed ripples (b) which can appear just after ($L = 10.4$ cm, $f = 1$ Hz, and $\Gamma_{water} = 0.35$). Deviation of the ''2/3 law'' (c) as a function of the relative acceleration parameter $\Gamma_{water} = \rho_{sand} a_i / (\rho_{sand} - \rho_{water}) g$. The scaling of images (a) and (b) is the same as in Fig. 2.

[Fig. 2(d)]. Note that small scale oscillations in the slope measurements [Figs. 2(b) and 2(d)] come from small irregularities in the granular interface. Also, we have noticed that even for weak amplitude ''rolling-grain'' ripples (one order of magnitude smaller than the final state) the slope could be locally close to its maximum value, as is shown in Fig. 2(b). Hence, the height and the shape of the sand pattern seem to be controlled by a large local slope at several stages of the evolution. Therefore, when the 2/3 law is satisfied, the amplitude of the final state is directly proportional to the fluid excursion L. For a wide range of parameters both the wavelength and the amplitude of ''vortex'' ripples are mainly controlled by L. The value of the maximum slope ($\varphi_{max} = 20° \pm 2°$) is slightly smaller than the minimum static angle of repose for a dry granular material composed of spherical glass particle. Either the density of the granular packing [10], the gap width of the channel [11] or the surface interaction in wet granular media may affect the value of this angle. Hence, we measured in our annular cell the static angle (angle of repose after avalanche) under water. For this, avalanches were obtained by sucking up glass particles from the sand bed with a large pipe having a diameter close to the gap width. We found a static angle under water of $25° \pm 1°$, which is very close to the value of $26°$ (static angle in air) obtained [11] for a rectangular cell having the same gap as our annular channel.

It is well known that, due to horizontal vibrations, sand liquefaction may occur in a sand-water cell [12]. For a sand-air system, a superficial fluidization of the sand layer appears [13] when the acceleration parameter $\Gamma_{air} = a_i / g$ reaches a

critical value around 0.55–0.65. However, the onset of liquefaction for the sand-water system has not yet been measured. Hence, we investigated how the shape and the mean wavelength of the final pattern evolve when Γ_{water} was increased. We observed that, for a given L, even if the mean wavelength λ remained constant (when the 2/3 law is satisfied) the shape of the final patterns depended slightly on the frequency. For small frequencies the ripple crests were sharper than the valleys, as shown in Fig. 2(c), but for higher frequencies the crests became smoother and almost sinusoidal ripples were obtained [see Fig. 4(a)]. Small oscillations of the crest, in phase with the periodic motion of the water, could be easily observed in this case and therefore ripple peaks tended to be smoothed. As shown in Fig. 4(c), a systematic deviation from the 2/3 law has been found above a critical value of $\Gamma_{water} \simeq 0.26$. For higher values of Γ_{water} the final wavelength was larger than the one predicted by the 2/3 law and ''squashed'' ripples could be obtained [see Fig. 4(b)]. In this regime, small propagating ripples appeared frequently on the surface of the large scale pattern. These small propagating ripples disappeared when the fluid motion was stopped. Hence, when the inertial acceleration a_i approached the effective gravity, the sand transport mechanism was strongly modified by the superficial liquefaction of the sand layer and a significant deformation affected both the shape and the wavelength of the final ripple state. Taking into account this fluidization mechanism may lead to a new interpretation of the wavelength transition, recently found by [6] for steep sand ripples when $\Gamma_{water} \simeq 0.27$ and $d = 110 \ \mu$m.

In conclusion, our results show that the evolution of sand ripples under an oscillatory flow can be very long and the final state corresponds to ''vortex'' ripples. The dynamical evolution of steep ripples obeys an inverse cascade mechanism which saturates at a given wavelength. The growth of the ripples appears to be limited only by the static angle of repose of the granular media. We have found that the final state exhibits a strong hysteresis and that relaxation from large to small wavelengths is not possible. These nonlinear behaviors should be taken into account in phenomenological models trying to reproduce the dynamic of steep ripples. Finally, for high inertial acceleration, the superficial fluidization of the sand layer affects both the wavelength and the shape of the final pattern.

[1] R.A. Bagnold, Proc. R. Soc. London, Ser. A **187**, 1 (1946).

[2] A. Kaneko and H. Honji, J. Fluid Mech. **93**, 727 (1979).

[3] P. Blondeaux, J. Fluid Mech. **218**, 1 (1990); G. Vittori and P. Blondeaux, *ibid.* **218**, 19 (1990).

[4] S.J.M.H. Hulscher, J. Geophys. Res. **101** (C9), 20 727 (1996); N.L. Komarova and S.J.M.H. Hulscher (unpublished); N.L. Komarova and A. Newell (unpublished).

[5] J.F.A. Sleath, J. Hydraul. Res. **14**, 69 (1976).

[6] M.A. Scherer, F. Melo, and M. Marder, Phys. Fluids A **11**, 58 (1999).

[7] P. Nielsen, J. Geophys. Res. **86** (C7), 6467 (1981).

[8] A. Betat, V. Frette, and I. Rehberg, Phys. Rev. Lett. **83**, 88 (1999).

[9] A. Aouidef, C. Normand, A. Stegner, and J.E. Wesfreid, Phys. Fluids **6**, 3665 (1994).

[10] J.R.L. Allen, Geol. Mijnbouw **49**, 13 (1970).

[11] Y. Grasselli and H.J. Herrmann, Physica A **246**, 301 (1997).

[12] A. Ivanova, V. Kozlov, and P. Evesque, Europhys. Lett. **35**, 159 (1996).

[13] G.H. Ristow, G. Straßburger, and I. Rehberg, Phys. Rev. Lett. **79**, 833 (1997); S.G.K. Tennakoon and R.P. Behringer, *ibid.* **81**, 794 (1998).

[14] K.H. Andersen, Ph.D. thesis, The Niels Bohr Institute, 1999 (unpublished), available at http://alf.nbi.dk/~kenand.